Experimental study of a nanoscale translocation ratchet

Bastien Molcrette, Léa Chazot-Franguiadakis, Zsombor Balassy, Céline Freton, Christophe Grangeasse, I D Fabien Montel

PNAS RESEARCH ARTICLE | BIOPHYSICS AND COMPUTATIONAL BIOLOGY

Experimental study of a nanoscale translocation ratchet

Bastien Molcrette[a], Léa Chazot-Franguiadakis[a], François Liénard[a], Zsombor Balassy[b], Céline Freton[c], Christophe Grangeasse[c], and Fabien Montel[a,1]

Edited by Steve Granick, Institute for Basic Science, Daejeon, South Korea; received February 11, 2022; accepted May 24, 2022

Despite an extensive theoretical and numerical background, the translocation ratchet mechanism, which is fundamental for the transmembrane transport of biomolecules, has never been experimentally reproduced at the nanoscale. Only the Sec61 and bacterial type IV pilus pores were experimentally shown to exhibit a translocation ratchet mechanism. Here we designed a synthetic translocation ratchet and quantified its efficiency as a nanopump. We measured the translocation frequency of DNA molecules through nanoporous membranes and showed that polycations at the *trans* side accelerated the translocation in a ratchet-like fashion. We investigated the ratchet efficiency according to geometrical and kinetic parameters and observed the ratchet to be only dependent on the size of the DNA molecule with a power law $N^{-0.6}$. A threshold length of 3 kbp was observed, below which the ratchet did not operate. We interpreted this threshold in a DNA looping model, which quantitatively explained our results.

translocation ratchet | zero-mode waveguide | nanopore | polymer translocation | biophysics

Significance

Some classes of biological motors like the Sec61 complex or the bacterial type IV pilus can achieve directional transport of biomolecules through nanopores, according to an out-of-equilibrium process called translocation ratchet, which biases thermal fluctuation toward a preferential direction. Despite its biological relevance, this process has never been reproduced into an artificial system. In this frame, we developed an artificial translocation ratchet at nanoscale, able to perform directional transport of DNA molecules through synthetic nanopores. We quantified the effect of both geometrical and kinetic parameters of this system on its ability to enhance the DNA transport and found the length of the DNA to be the main parameter likely to change the ratcheting effect; specifically, we observed a minimal length to trigger the ratchet mechanism that has never been described before.

The translocation ratchet, as a system with broken symmetry that biases Brownian fluctuations to achieve transport of macromolecules, is a ubiquitous process in biological pores, where a chemical gradient induces an asymmetry. This class of motors differs from other translocation motors like the bacteriophage packaging motor (1, 2) by its use of binding particles to rectify diffusion of macromolecules and induce a directional transport through the pore (3, 4). This has been experimentally shown for the complex Sec61 in its posttranslational pathway with eucaryotic cells, where chaperone proteins called BiP strongly attach to the translocating protein by ATPase activity (5); in the bacterial type IV pilus where ComEA chaperones bind to the DNA during its uptake and process its translocation into the bacterial periplasm in an ATP-independent translocation ratchet mechanism (6); or, recently, for the pore loops of ClpB, that display an ATP-dependent ratchet mechanism (7). Although experimental evidence has been provided for these systems, we lack a mechanistic investigation to describe quantitatively the translocation ratchet. Theoretical models (8–13) have been proposed since the Peskin and coworkers (3, 4) model, in which the translocation process of an infinite rod is driven by the binding equilibrium between the rod and binding particles at the *trans* side of the pore. Numerical studies have shown the relevance of such models to account for the experimental observations on the Sec61 complex and also pointed out a power stroke mechanism as a possible alternative mechanism to translocation ratchet, without the ability to distinguish between them (14, 15). In parallel, the influence of physical parameters on the translocation time of a polymer with a translocation ratchet has been investigated (8, 16–18). The effect of polymer length has been the main scope of these studies, showing similarities between the translocation ratchet and forced translocation (17, 18).

Based on this statement, we designed a nanoscale device that induced the directional transport of DNA through nanoporous membranes. This system has been developed upon a previous translocation setup (19) in which DNAs were forced through a 6-μm-thick nanoporous membrane with the help of a driving pressure between the *cis* and *trans* sides of the membrane and detected optically with a zero-mode waveguide (20). Polycations added at the *trans* side of the membrane prevented DNA backsliding through electrostatic binding, which created the translocation ratchet mechanism. The number of translocated DNA over time, called the translocation frequency (defined as the number of DNA molecules that entirely translocated from the *cis* to the *trans* side per unit time and normalized by the number of nanopores in the field of view) was measured by optical detection based on the zero-mode waveguide effect (see *DNA Preparation* for a complete description of our experimental setup).

Results

Preliminaries. The translocation experiment with an applied pressure was previously described by a theoretical model called the suction model, which predicts the frequency

Author contributions: B.M. and F.M. designed research; B.M., L.C.-F., F.L., Z.B., and C.F. performed research; C.F. and C.G. contributed new reagents/analytic tools; B.M. and F.M. analyzed data; and B.M. and F.M. wrote the paper.

The authors declare no competing interest.

This article is a PNAS Direct Submission.

[1]To whom correspondence may be addressed. Email: fabien.montel@ens-lyon.fr.

This article contains supporting information online at https://www.pnas.org/lookup/suppl/doi:10.1073/pnas.2202527119/-/DCSupplemental.

Published July 18, 2022.

of complete translocation of DNA molecules from the *cis* to the *trans* side of a nanopore as a function of the driving pressure between the two sides of the membrane (19, 21–23). The suction model applies to flexible or semiflexible polymers in dilute regime, with no attraction between the monomers and the nanopores, and whose radius of gyration is bigger than the radius of the nanopores. According to this model, the translocation frequency was related to the applied pressure as follows:

$$f = k\frac{P}{P_c}\exp\left(-\frac{P_c}{P}\right), \qquad [1]$$

with $P_c \propto R^{-4}Lk_BT$ a critical pressure (R is the radius of the nanopore, and L is its length) and k as a proportionality factor (per second) (see *SI Appendix* and refs. 19, 21, and 22 for further development of the suction model).

In the present study, the suction model has been used as the basis for a more complete model introducing the translocation ratchet mechanism.

Proof of Principle of the Translocation Ratchet. An increase of the translocation frequency was observed for all pressures after addition of polyethyleneimine (PEI), which was one of the polycations used in this study (see *Polycations*), with a magnitude that grew according to the pressure and the concentration of polycations (Fig. 1*B*); this concentration was expressed as the charge ratio ρ_+/ρ_- between the positive charge density ρ_+ of polycation and the negative charge density ρ_- of the DNA (see *Charge Ratio*). Measurements of the critical pressure P_c from Eq. **1** did not show significant changes by the addition of PEI (107 mbar with excess of PEI, 85 mbar without PEI) (*SI Appendix*, Fig. S4), which indicates that the presence of a ratchet agent at the exit of the nanopore did not change the energy barrier at the entrance. In a striking contrast, a quantitative increase of k was observed (Fig. 1*B*). The specificity of this increase with PEI has also been verified by the addition of heparin (negatively charged) in the *trans* side as a competitor to DNA for binding to polycations (24, 25) (*SI Appendix*, Fig. S3). The addition of heparin with PEI canceled the translocation enhancement effect of the polycation, and a significant similarity between the curves without PEI and with PEI/heparin was observed (*SI Appendix*, Fig. S3). This result ensured the polycation-specific enhancement of the DNA translocation, which cannot be attributed to an osmotic effect independent of the cationic nature of the species in solution.

We performed a statistical study of the noise on the translocation frequency measurements. Our results have shown that the event detection process was limited by Poisson noise coming from the random process of polymer capture by the nanopores; specifically, the optical detection was not the limiting process (see *SI Appendix* for a complete description of our noise study).

Ratchet Yield *Y*. According to Eq. **1**, the relative frequency increase by ratchet was defined as follows:

$$\frac{\Delta f}{f_{\rho=0}} = \frac{f_{\rho+} - f_{\rho=0}}{f_{\rho=0}}, \qquad [2]$$

with $f_{\rho+}(P)$ as the translocation frequency at a given concentration of polycations and $f_{\rho=0}(P)$ as the one without polycations. $\Delta f/f_{\rho=0}$ was measured as a function of the charge ratio for different species of polycations (Fig. 2*A*). A pressure-independent linear relation between $\Delta f/f_{\rho=0}$ and ρ_+ was observed for all polycations (Fig. 2*A*). The ratchet yield Y was introduced as $\Delta f/f_{\rho=0} = Y \times \rho_+/\rho_-$. Given this definition, we performed the translocation experiments with constant pressure and variable

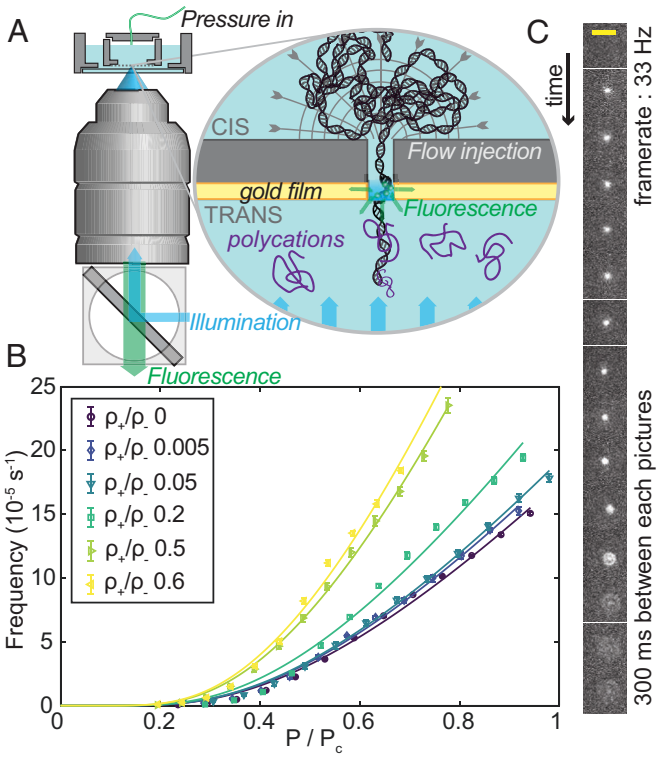

Fig. 1. Polycations accelerate DNA translocation. (*A*) Schematic representation of the experimental translocation ratchet observed by the zero-mode waveguide technique. (*B*) Frequency of λ DNA translocation as a function of the applied pressure (normalized by the critical pressure P_c) for variable concentrations of PEI (expressed as the charge ratio). Data are mean ±95% SEM fitted with the suction model Eq. **1** (lines); $n = 107$ (ρ_+/ρ_- 0), 12 (0.005), 20 (0.05), 12 (0.2), 47 (0.5), and 8 (0.6). (*C*) Time evolution of a flash caused by the translocation of a single fluorescently labeled DNA. (Scale bar: 6 μm.)

polycation concentrations (instead of the inverse), which led to a faster protocol to measure the ratchet yield Y (see *SI Appendix* for details and a comparison between the two methods).

The ratchet yield appeared to be constant for all polycations, with $Y \simeq 10$, except for PEI (pH 7.6): $Y_{PEI} \simeq 2.6$ (Fig. 2). This difference was understood by the incomplete protonation of PEI at physiologic pH (26), since Y (PEI, pH 4.3) was in the range of the other polycations (Fig. 2).

The dissociation constant K_d between λ DNA and the polycations was then measured by microscale thermophoresis (MST) (27, 28) and fluorescence decay methods (29, 30) (see *SI Appendix* and *SI Appendix*, Fig. S6 for complete details on fluorescence decay/MST experiments). These measurements were compared to the ratchet yields Y for each ratchet agent (Fig. 2*B*). From these observations, it appeared that Y did not evolve significantly with K_d, which implies a kinetic control of the binding between polycations and DNAs ($k_{off}/k_{on} \ll 1$) (31).

Effect of Geometrical Parameters on the Ratchet Yield.

Radius of the nanopore. The influence of the geometrical parameters on Y was studied. The first one was the radius of the nanopores R, which is a key parameter in translocation experiments. The translocation frequency of λ DNA was measured as a function of the applied pressure through nanopores with variable radii, from 25 nm to 100 nm (Fig. 3). Auger et al. (19) demonstrated that P_c is highly dependent on R with $P_c \propto R^{-4}$, which we also observed in our experiments both with and without ratchet in equal manner (Fig. 3*C*). The measurements of $\Delta f/f_{\rho=0}$ as a function of ρ_+ for variable R (Fig. 3 *A*, *B*, and *D*) showed an

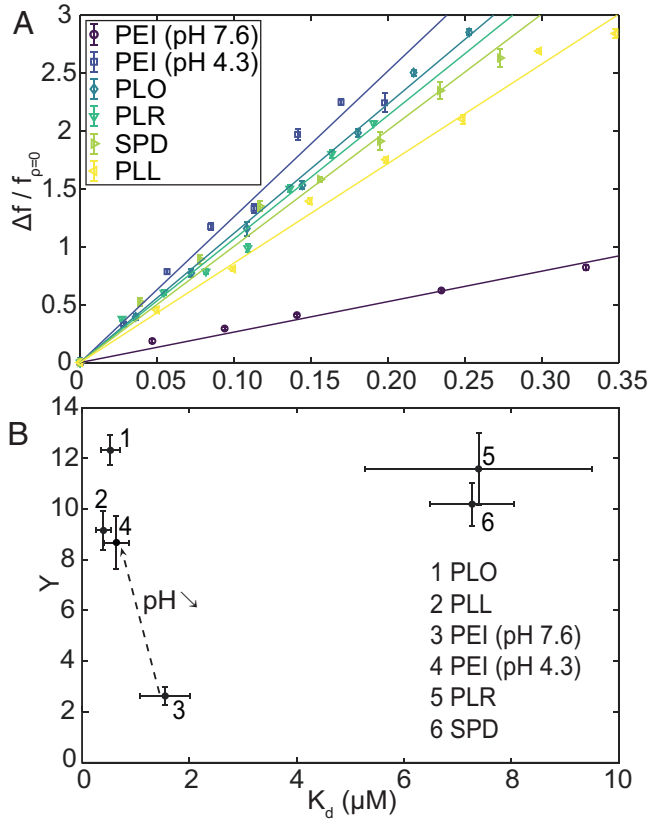

Fig. 2. Translocation ratchet is unspecific of the polycation. (*A*) Relative frequency increase by ratchet $\Delta f/f_{\rho=0}$ of λ DNA translocation as a function of the charge ratio with different polycations: PLO, PLL, PEI, PLR, and SPD. Experimental data were fitted by a linear regression model, and a ratchet yield Y was defined as the slope of the fit. (*B*) Ratchet yield Y as a function of the dissociation constant for different polycations. Data are mean ±95% SEM; $n = 47$ (PEI, pH 7.6) and 8 (others) for Y measurements; $n = 5$ (PLO), 4 (PLL), 4 (PEI, pH 4.3), 5 (PLR), and 4 (SPD) for K_d measurements.

increase of the translocation frequency with the addition of PEI for every size of nanopore, which meant the ratchet mechanism is valid at least in the range of 25 nm to 100 nm in radii. However, Y was shown to be independent of R in this range (Fig. 3 *D*, *Inset*), which highlighted that the ratchet agents did not influence the energy barrier at the entrance.

Length of the DNA molecule. Finally, the dependence of the ratchet mechanism on the contour length N of the DNAs was studied. The translocation experiments were realized at fixed pressure and variable concentrations of PEI with DNAs from 710 bp to 166 kbp. $\Delta f/f_{\rho=0}$ and Y were measured as a function of ρ_+/ρ_- (Fig. 4). No ratchet effect was observed for DNA smaller than 3 kbp. The ratchet mechanism was activated for DNAs above 3 kbp according to a scaling law $Y \propto N^{-\alpha}$ with $\alpha = 0.60 \pm 0.02$.

Phenomenological Model of the Translocation Ratchet. An extension of the suction model has been developed to explain the scaling observed for the physical parameters of the translocation ratchet. Given the adsorption rate of polycation on DNA (31) and the association time of 2 ns to 20 ns between DNA and polycations (PEI/poly-L-lysine [PLL]) measured from simulations at charge ratios 0.18 to 0.91 (32, 33), we assumed that the translocation of the polymer is the limiting step [the translocation duration was estimated to be around 0.2 s to 1 s from the flash duration (Movie S1) (19)]. The linear dependence between $\Delta f/f_{\rho=0}$ and ρ_+ can be explained with a two-step mechanism for the translocation (Fig. 5*A*): 1) The DNA is stopped by the nanopore and confined with a rate given by the suction model f_{suc}; 2) in the presence of ratchet agents, retrodiffusion of DNA will be inhibited once its extremity exits the nanopore. With typical values of 10^{-3} s to 10^{-2} s^{-1} for the dissociation rate between DNA and polycations (31), we considered that polycations remain bound to DNA during the entire translocation. We defined $p_{rat} \propto \rho_+/\rho_-$ as the probability for the DNA to find a ratchet agent, and defined $p_{\overline{rat}}$ as its complementary probability ($p_{\overline{rat}} = 1 - p_{rat}$). We also defined k_{rat} and $k_{\overline{rat}} < k_{rat}$ as the exit rates of DNA in the presence (k_{rat}) or absence ($k_{\overline{rat}}$), respectively, of ratchet agents. According to this two-step model, the linear dependence between the translocation frequency f and ρ_+ (Fig. 2*A*) was retrieved,

$$f \propto f_{suc} \times (p_{\overline{rat}} \times k_{\overline{rat}} + p_{rat} \times k_{rat}) \propto f_{suc} \times k_{\overline{rat}} \times \left[1 + p_{rat} \times \left(\frac{k_{rat}}{k_{\overline{rat}}} - 1\right)\right]. \quad [3]$$

In the regime of high efficiency of the ratchet ($k_{rat} \gg k_{\overline{rat}}$), we retrieved our experimental findings $f \propto f_{\rho=0} \times (1 + Y \times \rho_+/\rho_-)$, with $f_{\rho=0}$ as the translocation frequency without polycations and with the ratchet yield as $Y \propto k_{rat}/k_{\overline{rat}}$.

To explain the results with DNA contour length observed in our experiments (Fig. 4), we propose that the presence of bound ratchet agents could stabilize the formation of a DNA loop by thermal fluctuation, which would lead to a tension propagation along the DNA chain and a ratcheting process with ratchet step defined as the loop length (Fig. 5*B*). This loop model is supported by the fact that spermidine (SPD) operated as a ratchet while the molecule was much smaller than the diameter of the nanopores (Fig. 2*A*), which was counterintuitive for a translocation ratchet mechanism. Additionally, with an enthalpic cost of formation expressed as $2\pi^2 L_p/L_{loop}$ (in $k_B T$ units) (34), with L_p as the persistence length of DNA and L_{loop} as the length of the DNA loop, the minimal length of a DNA loop induced by thermal fluctuation of order $k_B T$ would be $L_{loop} = 2\pi^2 L_p \simeq 3$ kbp, hence the threshold observed in our experiments. The looping timescale of an interior loop stabilized by a polycation, of order 10^{-3} s to 10^{-2} s, is also in good agreement with a translocation duration of 0.1 s to 1 s (35). To further test our loop model, we measured the ratchet yield of 2.7-kbp DNA in buffer with a higher ionic strength (100 mM KCl, 10×), which decreased the persistence length of DNA and should decrease the critical length for the looping process, according to our model (Fig. 4). We observed that the increase of ionic strength triggered a ratchet effect for the 2.7-kbp DNA with $Y = 5.1 \pm 0.1$, which supports our loop model. Above 3 kbp, we assumed that k_{rat} is dominated by tension propagation dynamics (36–38): Given the enthalpic energy gain ΔG from the bond formation between polycation and DNA, measured by MST, $\Delta G = -log(K_d) \simeq 14 k_B T$, we assumed a strongly driven regime, $k_{rat} = k_B T/(N^{\nu+1}\eta a^3)$, with N as the number of monomers, η as the viscosity of the fluid, and a as the monomer size of the DNA. This hypothesis is supported by previous theoretical (36–38), numerical (17, 18), and experimental (39, 40) studies. We also measured this condensation force and the DNA looping by PLL with combined optical tweezers and confocal setup; specifically, we measured a tension force around 10 pN in the DNA chain during loop formation that supports our strongly driven regime hypothesis (see *SI Appendix* and Movie S2 for a complete discussion of our optical tweezers experiments). In the absence of ratchet, the exit rate of DNA $k_{\overline{rat}}$ is dominated by diffusion: $k_{\overline{rat}} = k_B T/(L^2 N \eta a)$, with L as the length of the pore. This implies $Y \simeq k_{rat}/k_{\overline{rat}} \propto (L/a)^2 \times N^{-\nu}$. In the frame of our loop model to trigger the ratchet (Fig. 5*B*), with

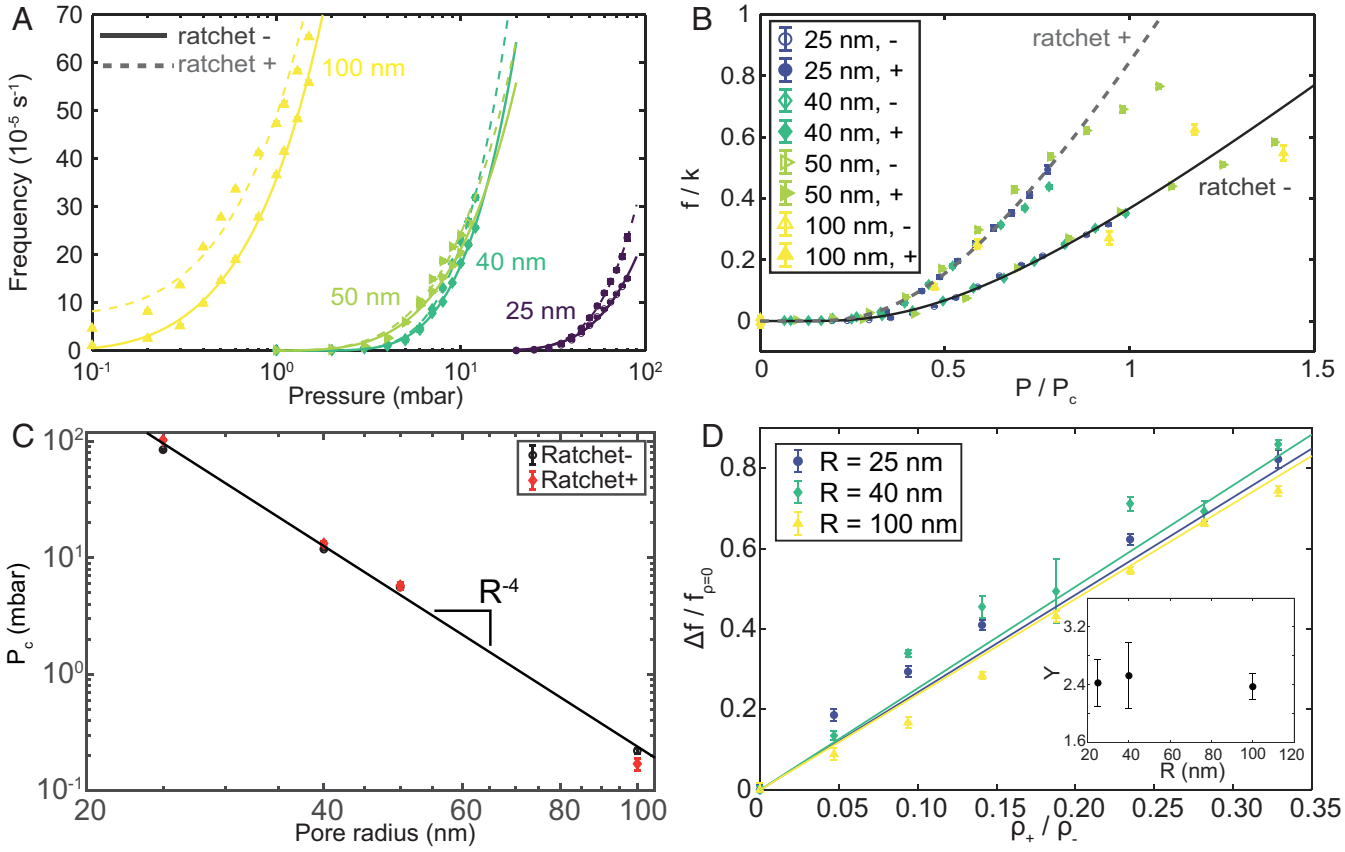

Fig. 3. Ratchet effect is independent of the nanopore radius. (*A*) Translocation frequency as a function of the driving pressure for different sizes of nanopore radius, with polycations (PEI, $\rho_+/\rho_- = 0.5$, ratchet+) or without (ratchet−). (*B*) Same as *A* but with pressure axis normalized by P_c and frequency axis normalized by k (from ratchet−) for each size of nanopore. (*C*) P_c as a function of the radius of the nanopores, with ratchet (PEI, $\rho_+/\rho_- = 0.5$) or without. (*D*) $\Delta f/f_{\rho=0}$ as a function of the charge ratio for different radii of nanopores. (*Inset*) Ratchet yield as a function of the nanopore radius. Data are mean ±95% SEM; $n = 107$ (ratchet−, 25 nm), 47 (ratchet+, 25 nm) and 8 (others). Fits correspond to the suction model Eq. **1** from which P_c was extracted.

a monomer size scaled as a DNA loop length ($\simeq 3$ kbp), this scaling argument is in excellent agreement with our results: It predicts the value of Y ($Y_{theo} = 6.5$; $Y_{exp} \simeq 10.4$, average over Fig. 2*B*). It also explains the experimental scaling law $Y \propto N^{-\alpha}$, with $\alpha = 0.6$ ($\alpha_{theo} \simeq 0.588$).

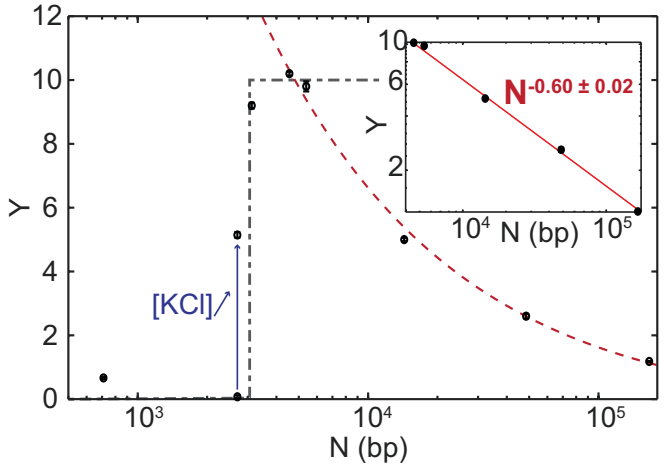

Fig. 4. Ratchet yield as a function of the DNA contour length. Data above 3 kbp have been fitted (red dashed line) according to a power law: $Y \propto N^{-0.6}$ (coefficient of determination, $R^2 = 0.996$), with a Heaviside function centered at 3 kbp (black dashed line). Blue data point corresponds to 2.7 kbp DNA in 100 mM KCl buffer (10×). (*Inset*) Log–log plot in the range 5 kbp to 166 kbp. Data are mean ±95% SEM; $n = 8$.

Discussion

This study is a proof of principle that ratchet agents can be used to enhance macromolecular transport through nanopores as previously proposed theoretically (4, 11). Contrary to previously reported artificial systems (41, 42), which used an asymmetric periodic channel or asymmetric periodic forcing, our methodology is based on a chemical gradient, which is closer to their biological counterparts. Our measurements have shown that the ratchet mechanism did not interfere with the energy barrier at the entrance of the nanopore in the frame of the suction model and operated, rather, downstream, which is supported by the observation of the independence of P_c with regard to the addition of polycations (*SI Appendix*, Fig. S4) and the fact that the ratchet yield Y did not change with the radius of the nanopore (Fig. 3). Specifically, it emphasizes that the ratchet effect is a stronger phenomenon than the pressure driving; otherwise, the ratchet yield would have depend on P_c. Moreover, with $Y \simeq k_{rat}/\overline{k_{rat}} \simeq 10$ (Fig. 2*B*), the addition of polycations at the exit of the nanopores enhanced the speed of the translocation by a factor of 10, which would have required an increase by 10 of the driving force in a purely pressure-driven translocation to get the same speed.

In contrast to voltage-driven setups, which have been the main translocation system used in recent years (43–46), pressure-driven translocation setups can generate smooth transitions between the purely diffusive regime to the strong driven regime of translocation, that makes it possible to measure a ratchet effect competing with the energy barrier at the entrance of the nanopore on an experimental timescale (19). Furthermore, a voltage-driven

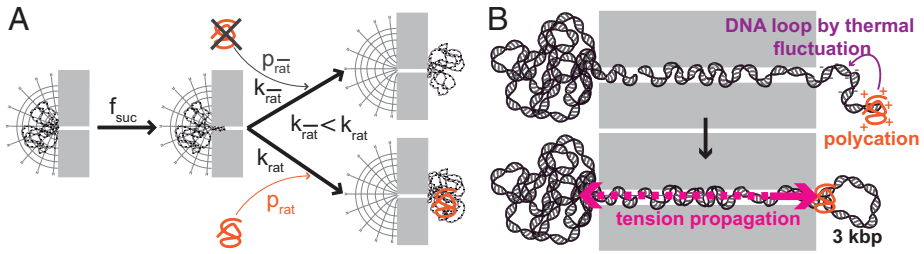

Fig. 5. DNA loops trigger the ratchet effect. (*A*) Kinetic model for the translocation of DNA with polycations: 1) confinement of the DNA into the nanopore according to the suction model with rate f_{suc}; 2) transport of the confined DNA toward the exit with a rate k_{rat} if the DNA is caught by a polycation (probability p_{rat}), or, otherwise, with a rate $k_{\overline{rat}} \ll k_{rat}$. (*B*) DNA loop model to trigger the ratchet effect: A spontaneous DNA loop (minimal size 3 kbp) is stabilized by a bound polycation, which generates a tension along the DNA chain and ratchets the translocation with a step equal to the loop length.

translocation would have inhibited the use of a cationic ratchet agent, because of the translocation of the polycation through the nanopore in the opposite direction to that of the DNA, thus canceling the ratchet effect.

Previous theoretical studies have shown that, in the large adsorption limit $k_{on} \gg k_{off}$, the ratchet yield evolves as $Y \propto L/\delta$, with L as the length of the polymer and δ as the ratchet step. In their models, they considered the free diffusion of a stiff rod through an infinitely thin nanopore. However, numerous theoretical and numerical studies have observed the relevance of the tension propagation theory to take into account the out-of-equilibrium nature of polymer translocation. Specifically, for translocations driven by binding particles, the Chuang–Kantor–Kardar (47) limit hypothesized the average translocation duration $\langle\tau\rangle$ to scale as $\langle\tau\rangle \propto N^{\nu+1}$, which has been numerically verified for long polymers ($N \simeq 10^6$). In our study, the tension propagation theory successfully led to the experimental scaling observed between the ratchet yield and the polymer size (Fig. 4), which could not be explained by models of translocation with the two sides of the polymer at equilibrium. Since most of the biological translocation ratchets operate with biopolymers (DNA, denatured proteins), our study emphasizes the need to take into account the polymer nature of the transported molecules to get a more accurate view of their transport through biological nanopores.

Another major aspect of our study is the evidence of a DNA length threshold to trigger the ratchet effect (Fig. 4), which has never been reported, to our knowledge. The clear threshold around 3 kbp and the fact that SPD enhanced the translocation despite its size being much smaller than the diameter of the nanopores (Fig. 2*A*) provide experimental insights that polycations generate a DNA complex of minimal size 3 kbp, which then accelerates the translocation in a ratchet-like mechanism. Previous studies have shown that polycations can generate DNA loops (48, 49), which has been extensively used to enhance DNA transfections (50). Given these experimental observations and the calculation of the enthalpic cost of a DNA loop as $2\pi^2 L_p/L_{loop}$, our DNA loop model can quantitatively explain our measurements. We assume that the loop regime could possibly be observed for two-dimensional (2D) or 3D simulations of semiflexible polymers translocation with multiple bonds ratchet agents in a low-concentration regime. In this case, the looping timescale would be shorter than the binding time for the ratchet agent.

We believe that our work will help to build a more accurate understanding of the key aspects of macromolecule transport in the cell. Specifically, this study highlights the influence of the length of the transported molecule and its mechanical properties. These parameters have not been investigated yet in biological pores like the nuclear pore complex, the bacterial type IV pilus, or the translocon. Finally, the present study paves the way to build new biomimetic nanopumps, which could be both selective and highly energy efficient.

Materials and Methods

DNA Preparation. For the translocated biopolymer, several DNAs have been used: λ DNA (48.5 kbp, ThermoFisher Scientific), λ DNA/HindIII (125 bp to 23,130 bp, average 14.3 kbp, New England Biolabs), T4 GT7 DNA (166 kbp, NIPPON GENE), Φ X174 RF II DNA (5.4 kbp, New England Biolabs), pNEB206A linearized (2.7 kbp, New England Biolabs), pCLIP$_f$-H2B (6.2 kbp, circular DNA, New England Biolabs), pKLAC2 (9.1 kbp, circular DNA, New England Biolabs), and DNA ladder (100 bp to 1,517 bp, average 710 bp, New England Biolabs). The concentration of DNA was kept constant at 4.9 nM (in phosphate groups equivalent) in buffer Tris-KCl (10 mM) and (ethylenedinitrilo)tetraacetic acid (1 mM) at pH 7.6 (25 °C). The DNAs have been fluorescently labeled with YOYO-1 (ThermoFisher Scientific) at 3.0 nM (about one YOYO-1 molecule available per DNA base).

Polycations. Polycations have been added to the downstream side of the membrane (*trans* side) at concentrations of a few micromolars (in nitrogen groups equivalent). We assumed that these ratchet agents bind to the DNAs at the exit of the nanopores and prevent the retrodiffusion of the transported molecules (Fig. 1*A*). The polycations used as ratchet agents were PEI (M.n. 60,000 g/mol, ACROS Organics), PLL (M.w. 150,000 g/mol to 300,000 g/mol, Sigma-Aldrich), poly-L-ornithine (PLO) (M.w. 147,000 g/mol, Sigma-Aldrich), poly-L-arginine (PLR) (M.w. 146,000 g/mol, Sigma-Aldrich), and SPD (Sigma-Aldrich).

Charge Ratio. The charge ratio ρ_+/ρ_- was defined as the ratio between average positive charge density ρ_+ from polycations in *trans* side bulk over the average negative charge density ρ_- in a DNA coil (worm-like chain model, $L_p = 50$ nm, two negative charges per base pair). This definition of the charge ratio was motivated by the assumption that binding between translocated DNA and polycations at the exit of the nanopores was not affected by the DNA bulk concentration at the *cis* side but by the local negative charge density at the exit of the nanopores (Fig. 1*A*).

Zero-Mode Waveguide Detection of DNA Translocation. To visualize the translocation of DNAs through the nanopores, a near-field microscopy technique based on the zero-mode waveguide effect was designed (Fig. 1*A*). A 50-nm gold layer was sputtered onto track-etched membranes (Whatman Nuclepore, 6-μm-thick polycarbonate, pore diameters between 50 and 200 nm) with an evaporator (EVA 300 Alliance Concept). An evanescent field (typical length: 43 nm) was created in the gold layer when excited by a 473-nm laser (Cobolt Blues), and the field was enhanced in the nanopores by plasmon resonance and an antenna effect due to the waveguide geometry of the nanopores. Thus, the fluorescence of the DNAs was only activated in the vicinity of the edge of the nanopores by the evanescent field (the *cis* side of the membrane was not illuminated, and YOYO-1 molecules were bleached at the *trans* side by the intensity of the light). With this experimental setup, the translocation of a DNA molecule was detected by a flash of light when the molecule crossed the exit of the nanopore (gold side) (Movie S1).

Image Acquisition. The membrane was glued onto a cap with biocompatible silicon glue (Silicomet JS 533, Loctite), and the DNAs were forced into the

nanopores by application of a gradient of pressure between the two sides of the membrane thanks to a pressure controller connected to the cap (Fluigent MFCS, 0 mbar to 1,000 mbar with 0.1-mbar resolution). The *trans* side of the membrane (where DNAs exit the nanopores through the gold layer) was visualized with an epifluorescence microscope (Zeiss Axiovert 200, water objective Zeiss ×63 C-Apochromat, NA 1.2), and images were acquired with an camera (iXon 897 Andor, −60 °C, 512 × 512 px^2). Several movies were recorded at 33 frames per second with 250 frames (see *SI Appendix* for a complete description of image/data processing, and see Movie S1 for an example of a typical translocation movie; Fig. 1*C* shows snapshots of a translocation event).

The frequency of translocation was measured as a function of the applied pressure with variable concentrations of PEI (50–52) as the ratchet agent, expressed as the charge ratio ρ_+/ρ_-.

Image Processing. The background noise was subtracted to enhance the signal detection (homemade ImageJ script), and the translocation events were manually counted (typically, around a hundred events for a movie); this process was repeated at least four times for each experimental condition. The frequency–pressure curves were processed by a homemade MATLAB (Mathworks) script, and the Curve Fitting Toolbox was used to fit these experimental curves. CIs of the fitting parameters were obtained by the Jackknife method (resampling method without replacement).

Data Availability. Microscopy movies are available in Zenodo (53). All other data are included in the article and/or supporting information.

ACKNOWLEDGMENTS. We thank Martin Castelnovo, Vincent Démery, Murugappan Muthukumar, and Christophe Ybert for fruitful discussions.

Author affiliations: [a]Laboratoire de Physique, CNRS UMR 5672, Université Claude Bernard, Ecole Normale Supérieure de Lyon, Université de Lyon, F-69342 Lyon, France; [b]LUMICKS, 1059 CH Amsterdam, The Netherlands; and [c]Laboratoire de Microbiologie Moléculaire et Biochimie Structurale, CNRS UMR 5086, Université de Lyon, 69007 Lyon, France

1. Y. R. Chemla *et al.*, Mechanism of force generation of a viral DNA packaging motor. *Cell* **122**, 683–692 (2005).
2. Z. T. Berndsen, N. Keller, S. Grimes, P. J. Jardine, D. E. Smith, Nonequilibrium dynamics and ultraslow relaxation of confined DNA during viral packaging. *Proc. Natl. Acad. Sci. U.S.A.* **111**, 8345–8350 (2014).
3. S. M. Simon, C. S. Peskin, G. F. Oster, What drives the translocation of proteins? *Proc. Natl. Acad. Sci. U.S.A.* **89**, 3770–3774 (1992).
4. C. S. Peskin, G. M. Odell, G. F. Oster, Cellular motions and thermal fluctuations: The Brownian ratchet. *Biophys. J.* **65**, 316–324 (1993).
5. K. E. Matlack, B. Misselwitz, K. Plath, T. A. Rapoport, BiP acts as a molecular ratchet during posttranslational transport of prepro-alpha factor across the ER membrane. *Cell* **97**, 553–564 (1999).
6. C. Hepp, B. Maier, Kinetics of DNA uptake during transformation provide evidence for a translocation ratchet mechanism. *Proc. Natl. Acad. Sci. U.S.A.* **113**, 12467–12472 (2016).
7. H. Mazal, M. Iljina, I. Riven, G. Haran, Ultrafast pore-loop dynamics in a AAA+ machine point to a Brownian-ratchet mechanism for protein translocation. *Sci. Adv.* **7**, eabg4674 (2021).
8. R. Zandi, D. Reguera, J. Rudnick, W. M. Gelbart, What drives the translocation of stiff chains? *Proc. Natl. Acad. Sci. U.S.A.* **100**, 8649–8653 (2003).
9. T. Ambjörnsson, M. A. Lomholt, R. Metzler, Directed motion emerging from two coupled random processes: Translocation of a chain through a membrane nanopore driven by binding proteins. *J. Phys. Condens. Matter* **17**, S3945–S3964 (2005).
10. M. R. D'Orsogna, T. Chou, T. Antal, Exact steady-state velocity of ratchets driven by random sequential adsorption. *J. Phys. Math. Gen.* **40**, 5575–5584 (2007).
11. PL Krapivsky, K Mallick, Fluctuations in polymer translocation. *J. Stat. Mech. Theory Exp.* **2010**, P07007 (2010).
12. A. Depperschmidt, N. Ketterer, P. Pfaffelhuber, A Brownian ratchet for protein translocation including dissociation of ratcheting sites. *J. Math. Biol.* **66**, 505–534 (2013).
13. D. Mondal, M. Muthukumar, Ratchet rectification effect on the translocation of a flexible polyelectrolyte chain. *J. Chem. Phys.* **145**, 084906 (2016).
14. W. Liebermeister, T. A. Rapoport, R. Heinrich, Ratcheting in post-translational protein translocation: A mathematical model. *J. Mol. Biol.* **305**, 643–656 (2001).
15. T. C. Elston, The Brownian ratchet and power stroke models for posttranslational protein translocation into the endoplasmic reticulum. *Biophys. J.* **82**, 1239–1253 (2002).
16. W. Yu, K. Luo, Chaperone-assisted translocation of a polymer through a nanopore. *J. Am. Chem. Soc.* **133**, 13565–13570 (2011).
17. R. Adhikari, A. Bhattacharya, Translocation of a semiflexible polymer through a nanopore in the presence of attractive binding particles. *Phys. Rev. E Stat. Nonlin. Soft Matter Phys.* **92**, 032711 (2015).
18. P. M. Suhonen, R. P. Linna, Chaperone-assisted translocation of flexible polymers in three dimensions. *Phys. Rev. E* **93**, 012406 (2016).
19. T. Auger *et al.*, Zero-mode waveguide detection of flow-driven DNA translocation through nanopores. *Phys. Rev. Lett.* **113**, 028302 (2014).
20. M. J. Levene *et al.*, Zero-mode waveguides for single-molecule analysis at high concentrations. *Science* **299**, 682–686 (2003).
21. C. Gay, P. G. de Gennes, E. Raphaël, F. Brochard-Wyart, Injection threshold for a statistically branched polymer inside a nanopore. *Macromolecules* **29**, 8379–8382 (1996).
22. T. Sakaue, E. Raphaël, P. G. de Gennes, F. Brochard-Wyart, Flow injection of branched polymers inside nanopores. *Eur. Lett.* **72**, 83–88 (2005).
23. T. Auger, L. Auvray, J. M. Di Meglio, F. Montel, Uncooked spaghetti in a colander: Injection of semiflexible polymers in a nanopore. *Eur Phys J E Soft Matter* **41**, 63 (2018).
24. I. Moret *et al.*, Stability of PEI-DNA and DOTAP-DNA complexes: Effect of alkaline pH, heparin and serum. *J. Control. Release* **76**, 169–181 (2001).
25. J. P. Clamme, J. Azoulay, Y. Mély, Monitoring of the formation and dissociation of polyethylenimine/DNA complexes by two photon fluorescence correlation spectroscopy. *Biophys. J.* **84**, 1960–1968 (2003).
26. K. Utsuno, H. Uludağ, Thermodynamics of polyethylenimine-DNA binding and DNA condensation. *Biophys. J.* **99**, 201–207 (2010).
27. M. Jerabek-Willemsen *et al.*, Microscale thermophoresis: Interaction analysis and beyond. *J. Mol. Struct.* **1077**, 101–113 (2014).
28. C. J. Wienken, P. Baaske, U. Rothbauer, D. Braun, S. Duhr, Protein-binding assays in biological liquids using microscale thermophoresis. *Nat. Commun.* **1**, 100 (2010).
29. M. X. Tang, F. C. Szoka, The influence of polymer structure on the interactions of cationic polymers with DNA and morphology of the resulting complexes. *Gene Ther.* **4**, 823–832 (1997).
30. D. S. Chu, J. G. Schellinger, M. J. Bocek, R. N. Johnson, S. H. Pun, Optimization of Tet1 ligand density in HPMA-co-oligolysine copolymers for targeted neuronal gene delivery. *Biomaterials* **34**, 9632–9637 (2013).
31. H. Torigoe, A. Ferdous, H. Watanabe, T. Akaike, A. Maruyama, Poly(L-lysine)-graft-dextran copolymer promotes pyrimidine motif triplex DNA formation at physiological pH. Thermodynamic and kinetic studies. *J. Biol. Chem.* **274**, 6161–6167 (1999).
32. J. Ziebarth, Y. Wang, Molecular dynamics simulations of DNA-polycation complex formation. *Biophys. J.* **97**, 1971–1983 (2009).
33. D. A. Kondinskaia, A. Y. Kostritskii, A. M. Nesterenko, A. Y. Antipina, A. A. Gurtovenko, Atomic-scale molecular dynamics simulations of DNA–polycation complexes: Two distinct binding patterns. *J. Phys. Chem. B* **120**, 6546–6554 (2016).
34. A. V. Drozdetski, A. Mukhopadhyay, A. V. Onufriev, Strongly bent double-stranded dna: Reconciling theory and experiment. *Front. Phys.* **7**, 10.3389/fphy.2019.00195 (2019).
35. C. Hyeon, D. Thirumalai, Kinetics of interior loop formation in semiflexible chains. *J. Chem. Phys.* **124**, 104905 (2006).
36. Y. Kantor, M. Kardar, Anomalous dynamics of forced translocation. *Phys. Rev. E Stat. Nonlin. Soft Matter Phys.* **69**, 021806 (2004).
37. T. Sakaue, Nonequilibrium dynamics of polymer translocation and straightening. *Phys. Rev. E Stat. Nonlin. Soft Matter Phys.* **76**, 021803 (2007).
38. J. Sarabadani, T. Ikonen, T. Ala-Nissila, Iso-flux tension propagation theory of driven polymer translocation: The role of initial configurations. *J. Chem. Phys.* **141**, 214907 (2014).
39. Y. J. Yang *et al.*, Cytosine methylation enhances DNA condensation revealed by equilibrium measurements using magnetic tweezers. *J. Am. Chem. Soc.* **142**, 9203–9209 (2020).
40. T. Quail *et al.*, Force generation by protein–DNA co-condensation. *Nat. Phys.* **17**, 1007–1012 (2021).
41. J. Bader *et al.*, A Brownian-ratchet DNA pump with applications to single-nucleotide polymorphism genotyping. *Appl. Phys., A Mater. Sci. Process.* **75**, 275–278 (2002).
42. M. Chinappi *et al.*, Molecular dynamics simulation of ratchet motion in an asymmetric nanochannel. *Phys. Rev. Lett.* **97**, 144509 (2006).
43. A. Meller, L. Nivon, D. Branton, Voltage-driven DNA translocations through a nanopore. *Phys. Rev. Lett.* **86**, 3435–3438 (2001).
44. Q. Liu *et al.*, Voltage-driven translocation of DNA through a high throughput conical solid-state nanopore. *PLoS One* **7**, e46014 (2012).
45. C. Plesa *et al.*, Fast translocation of proteins through solid state nanopores. *Nano Lett.* **13**, 658–663 (2013).
46. C. Wang, S. Sensale, Z. Pan, S. Senapati, H. C. Chang, Slowing down DNA translocation through solid-state nanopores by edge-field leakage. *Nat. Commun.* **12**, 140 (2021).
47. J. Chuang, Y. Kantor, M. Kardar, Anomalous dynamics of translocation. *Phys. Rev. E Stat. Nonlin. Soft Matter Phys.* **65**, 011802 (2002).
48. R. Golan, L. I. Pietrasanta, W. Hsieh, H. G. Hansma, DNA toroids: Stages in condensation. *Biochemistry* **38**, 14069–14076 (1999).
49. B. van den Broek *et al.*, Visualizing the formation and collapse of DNA toroids. *Biophys. J.* **98**, 1902–1910 (2010).
50. E. Bertrand *et al.*, Histidinylated linear PEI: A new efficient non-toxic polymer for gene transfer. *Chem. Commun. (Camb.)* **47**, 12547–12549 (2011).
51. A. Baker *et al.*, Polyethylenimine (PEI) is a simple, inexpensive and effective reagent for condensing and linking plasmid DNA to adenovirus for gene delivery. *Gene Ther.* **4**, 773–782 (1997).
52. S. Choosakoonkriang, B. A. Lobo, G. S. Koe, J. G. Koe, C. R. Middaugh, Biophysical characterization of PEI/DNA complexes. *J. Pharm. Sci.* **92**, 1710–1722 (2003).
53. B. Molcrette et al., Catch and thread: Experimental study of a nanoscale translocation ratchet. Zenodo. https://doi.org/10.5281/zenodo.6802447. Deposited 6 July 2022.